

Time-Domain Observation of External Magnetic Field Effects on the Delayed Fluorescence of *N,N,N',N'*-Tetramethyl-1,4-phenylenediamine in Alcoholic Solution

Yohei Iwasaki,[†] Kiminori Maeda,[‡] and Hisao Murai*

Department of Chemistry, Graduate School of Science, Tohoku University, Sendai 980-8578, Japan

Received: June 5, 2000; In Final Form: November 5, 2000

The external magnetic field effects (MFEs) on the intensity of the delayed fluorescence from *N,N,N',N'*-tetramethyl-1,4-phenylenediamine (TMPD) are studied in mixed alcohol and 2-propanol under the conditions of both low and high concentration of TMPD at room temperature. In mixed alcohol solution, three different MFEs on the delayed fluorescence intensity are separated by time-domain observation and different concentration conditions. The MFEs in the solution of low concentration can be explained by the radical-pair mechanism (RPM) of the TMPD cation radical and the solvated electron in the early-time region and the triplet-triplet pair mechanism (TTPM) through triplet-triplet annihilation (T-T annihilation) in the later-time region. In the solution of high concentration, the MFEs can be explained by the TTPM in the early-time region and the triplet-doublet pair mechanism (TDPM) in the later-time region. This TDPM affects the delayed fluorescence intensity of T-T annihilation. In 2-propanol, similar results are obtained, except for no apparent observation of the RPM. According to the present results, it is clarified that TMPD in alcohol emits two types of the delayed fluorescence, recombination type and T-T annihilation type. The former shows the MFEs due to the RPM, and the latter shows the two different MFEs of the TTPM and the TDPM.

Introduction

Many photochemical reactions take place through pairs of intermediate paramagnetic species in liquid media. In particular, radical pairs are well-known as one of the most important types of chemical intermediates because the spin selectivity of the reaction and intersystem crossing in the radical pair determine the reaction pathway. This has been investigated by observations of the external magnetic field effects (MFEs) on the chemical reaction yield, time-resolved electron spin resonance, and time-resolved reaction yield detected magnetic resonance techniques.^{1,2} The other kinds of pairs, a triplet-doublet pair and a triplet-triplet pair, might also play roles in photochemical reaction processes.

In some cases, delayed fluorescence is useful for the study of the pairs of paramagnetic species. The delayed fluorescence is classified into three types according to the mechanism of the occurrence of the lowest singlet excited state (S_1).^{3–6} The first is due to the thermal depopulation of the lowest excited triplet state (T_1) to S_1 . The second is caused by the interaction between two excited triplet-state molecules, which is called the triplet-triplet annihilation (T-T annihilation) type of delayed fluorescence. The third is recombination-type delayed fluorescence, which is due to the charge recombination of a cation and a solvated electron formed in solution. The MFEs on the delayed fluorescence in liquid media are usually attributed to the three pair mechanisms, the radical pair mechanism (RPM),^{1,2} the (excited) triplet-triplet pair mechanism (TTPM),^{1,3,4} and the (excited) triplet-doublet pair mechanism (TDPM).^{1,3,4} The RPM can be explained by the influence of the magnetic field on

singlet-triplet mixing through the hyperfine coupling mechanism (HFCM) and so on.^{1,2} The TTPM and TDPM can also be explained, respectively, by the influence of the magnetic field on the singlet-quintet and the doublet-quartet transitions induced by intradipole interactions of the excited triplet molecules.^{1,3,4} The recombination-type delayed fluorescence, which emits via the radical pair, shows the MFEs due to the RPM. The T-T annihilation type of delayed fluorescence, which emits via the T-T pair, shows the MFEs due to the TTPM. If both the triplet molecule and the doublet species have lifetimes long enough that they encounter each other, the T-T annihilation type of delayed fluorescence might also provide information on the TDPM. The thermal depopulation type of delayed fluorescence shows no external magnetic field effect in liquid media, because there exist no apparent pair-like spin-related interactions.

N,N,N',N'-Tetramethyl-1,4-phenylenediamine (TMPD) is known to be easily photoionized in alcoholic media.⁷ Hirata and co-workers showed that this photoionization process occurs by way of a long-lived transient species such as a radical-ion pair (RIP) of the TMPD cation radical and the solvated electron formed from the lowest excited singlet state of TMPD using a transient optical absorption technique and a photocurrent measurement.^{8,9} Tanimoto and co-workers showed the MFE on the transient photoconductivity in the system of TMPD in 2-propanol.¹⁰ The photoconductivity is proportional to the total amount of free ions created by escape from the RIP, and the MFE appears by singlet-triplet mixing in the RIP. We reproduced their results^{11,12} and succeeded in observing the photoconductivity-detected magnetic resonance (PCDMR)^{11,12} and the transient absorption-detected magnetic resonance (ADMR).¹² These results indicate that the predominant quenching manifold of the RIP is the triplet state in this particular system. Percy and co-workers showed the fluorescence-detected magnetic resonance (FDMR) spectrum observed in the photolysis of this system.^{13,14} They showed that the fluorescent state is formed by the

* To whom correspondence should be addressed. Fax: +81-22-217-6570. E-mail: murai@orgphys.chem.tohoku.ac.jp.

[†] Present address: Institute for Chemical Reaction Science, Tohoku University, Sendai 980-8577, Japan.

[‡] Present address: Department of Chemistry, University of Tsukuba, Tsukuba, Ibaraki 305-8571, Japan.

recombination of the singlet RIP created by biphotonic excitation of TMPD. We also tried to observe the FDMR signal and confirmed that the precursor was the highly excited singlet state of TMPD.¹⁵ In that investigation, the quantum nutation due to the microwave field was carefully studied at room temperature. We suggested that there existed not only the recombination-type delayed fluorescence but also another emission, which might be the T–T annihilation type of delayed fluorescence. However Sacher and Grampp have recently reported no MFEs by fluorescence detection in this system;¹⁶ our system provided apparent and peculiar MFEs that might be related to the spin of this particular system.

In this paper, new findings of the MFEs on the delayed fluorescence in the system of TMPD in mixed alcohol and 2-propanol are presented, and a discussion and rationalization of these findings are given.

Experimental Section

TMPD supplied by Aldrich Chemical was purified by vacuum sublimation. Special-grade 2-propanol and 2-methyl-2-propanol provided by Kanto Chemical were used as received. In the present system, a mixed alcohol solution (2-propanol/2-methyl-2-propanol ratio of 1:4 by volume) and a neat 2-propanol solution were deoxygenated by bubbling with pure nitrogen gas prior to and during the experiments. The solution was pumped through a flat quartz cell installed in an X-band ESR cavity (TE₀₁₁) and excited by an excimer laser (Lambda Physik, LPX-105, XeCl, $\lambda = 308$ nm) pulse under an external magnetic field (0–800 mT) at room temperature. The flow rate of the solution was about 8 mL min⁻¹, and the laser repetition rate was 20 Hz. The fluorescence was introduced to a photomultiplier tube (Hamamatsu, R1477) with a magnetic field shield case by an optical fiber with a Pyrex glass filter, which cuts off the direct laser light scatter. The signal detected by the photomultiplier tube was sent to a digital oscilloscope (LeCroy 9430) connected with a microcomputer system for data processing. The detail of this setup designed for our FDMR works was presented before.^{12,15}

The experiments were performed for two typical concentrations of the TMPD, 5×10^{-4} mol dm⁻³ (low concentration) and 1×10^{-2} mol dm⁻³ (high concentration), to clarify the mechanism of the MFEs.

Results and Discussion

Low-Concentration Experiment in Mixed Alcohol Solution. Figure 1a shows the time profile of the MFEs on the delayed fluorescence intensity, $[I(800 \text{ mT}) - I(0 \text{ mT})]/I(0 \text{ mT})$, under the low-concentration conditions in the mixed alcohol solution. Here, $I(800 \text{ mT})$ and $I(0 \text{ mT})$ are the delayed fluorescence intensities at 800 and 0 mT, respectively. The time region of 0–120 ns after the laser excitation is a dead time because of interruption of the observation by prompt fluorescence (lifetime ≈ 8 ns)⁸ with a strong intensity. The sign of the intensity ratio (sign of the MFE) changes from positive to negative at about 400 ns after laser excitation. This change suggests that multiple MFE mechanisms might exist. Figure 1b shows the magnetic field dependence (MFE curves) of the delayed fluorescence intensity ratio, $[I(B) - I(0 \text{ mT})]/I(0 \text{ mT})$, versus the external magnetic field strength (B) at 150 and 800 ns after laser excitation. The intensity ratio at 150 ns after laser excitation sharply increases with increasing external magnetic field up to about 40 mT, where it reaches a near plateau. At 800 ns after laser excitation, no obvious MFE is observed below about 100 mT, but the intensity ratio seems to gradually decrease

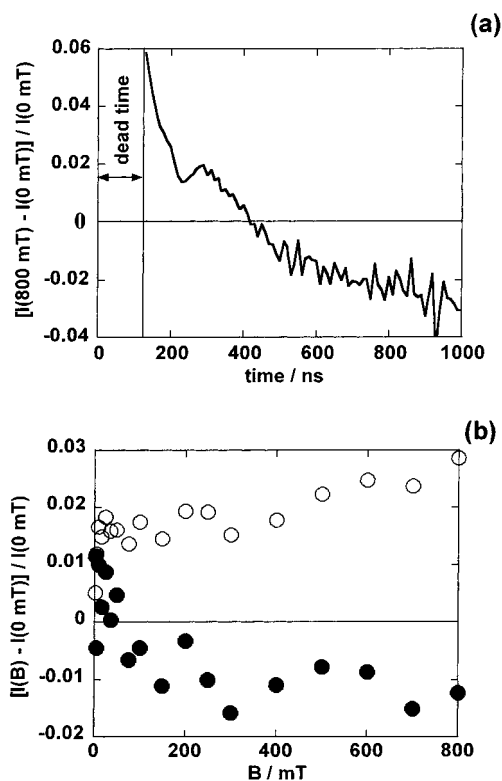


Figure 1. MFEs in mixed alcohol under the low-concentration conditions of TMPD (5×10^{-4} M) at room temperature. (a) Time-evolution of the intensity ratio $[I(B) - I(0 \text{ mT})]/I(0 \text{ mT})$ where $B = 800$ mT. The positive and negative signs of the intensity ratio show the increment and decrement of the delayed fluorescence intensity, respectively. (b) External magnetic field dependence of the intensity ratio. The open and closed circles show the field dependence at 150 and 800 ns after laser excitation, respectively.

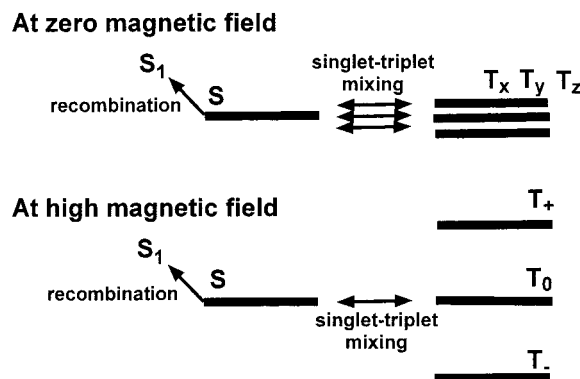


Figure 2. Conceptual diagram of the MFE due to the RPM. The singlet state (S), which is related to the recombination-type delayed fluorescence, can mix three triplet sublevels (T_x, T_y, T_z) at zero magnetic field but can mix only one triplet sublevel (T₀) at high magnetic field.

with increasing external magnetic field. The MFE in the early-time region is very similar to that observed in the photoconductivity measurements by Tanimoto et al.¹⁰ and our group^{11,12} and can be explained by the RPM.^{1,2} The positive sign of the MFE shows that the singlet precursor creates the singlet RIP.^{1,2} This is because the singlet state (S) of the RIP can mix three triplet sublevels (T_x, T_y, T_z) of the RIP at zero magnetic field but can mix only one triplet sublevel (T₀) of the RIP at high magnetic field, as shown in Figure 2. Therefore, the population of the singlet state of RIP at high magnetic field is greater than that at zero magnetic field, and the recombination-type delayed fluorescence intensity, which is proportional to the population of the singlet state of the RIP, increases with increasing B .

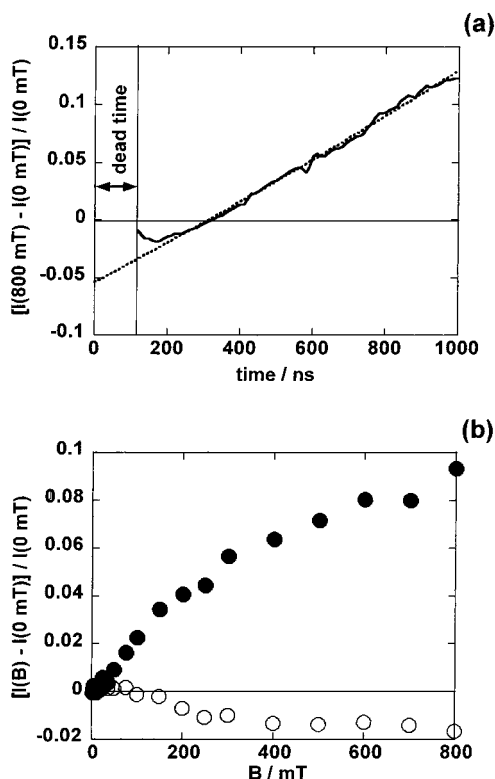


Figure 3. MFEs in mixed alcohol under the high-concentration conditions of TMPD (1×10^{-2} M) at room temperature. (a) The solid line shows the time-evolution of the intensity ratio $[I(B) - I(0 \text{ mT})]/I(0 \text{ mT})$ where $B = 800$ mT. The positive and negative signs of the intensity ratio show the increment and decrement of the delayed fluorescence intensity, respectively. The dotted line shows the curve fitting by eq 9. (b) External magnetic field dependence of the intensity ratio. The open and closed circles show the field dependence at 150 and 800 ns after laser excitation, respectively.

Because the main contribution of this singlet–triplet mixing is the HFCM, the specific parameter of $B_{1/2}$, which is the magnetic field strength at which the MFE reaches one-half the amplitude at the plateau, can be used as a measure of the HFCM.^{1,2} The value of $B_{1/2}$ defined theoretically by Weller et al. is¹⁷

$$B_{1/2} = \frac{2(B_a^2 + B_b^2)}{B_a + B_b} \quad (1)$$

where

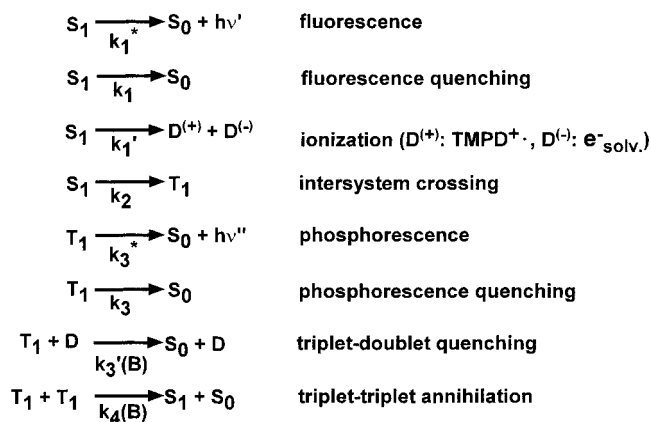
$$B_i = \left[\sum_j I_{ij}(I_{ij} + 1)A_{ij}^2 \right]^{1/2} \quad (i = a, b) \quad (2)$$

and j represents every magnetic nucleus contained in a radical pair. Assuming that the MFE curve reaches a plateau at 800 mT, the observed $B_{1/2}$ value is estimated to be about 5 mT. This value is close to the theoretical one of 3.2 mT estimated from the HFC constants.¹³

The MFE in the later-time region cannot be explained by the RPM. This MFE is discussed with regard to high-concentration experiment.

High-Concentration Experiment in Mixed Alcohol Solution. The solid line in Figure 3a shows the time profile of the delayed fluorescence intensity ratio for 800 mT and zero field, $[I(800 \text{ mT}) - I(0 \text{ mT})]/I(0 \text{ mT})$, under high-concentration conditions in the mixed alcohol solution. The sign of the MFE changes from negative to positive at about 300 ns after laser excitation. Figure 3b shows the MFE curves of the delayed

SCHEME 1



fluorescence intensity ratio for 150 and 800 ns after laser excitation. At 150 ns after laser excitation, no obvious MFE was observed from 0 to about 100 mT, but the intensity ratio gradually decreased with increasing external magnetic field. This MFE curve is similar to that observed in the later-time region under low-concentration conditions. The intensity ratio at 800 ns after laser excitation gradually increases with increasing external magnetic field. These MFEs cannot be simply explained by the RPM. Because the lifetime of the excited triplet state of TMPD is long enough to create the T–T pair,¹⁸ we can interpret them in terms of the T–T annihilation type of delayed fluorescence suggested in our previous paper.¹⁵ Here, we employed an analysis of the kinetics of the T–T annihilation process according to the treatment proposed by Azumi et al.¹⁹ The photochemical reactions of TMPD are postulated as shown in Scheme 1. $k_3'(B)$ and $k_4(B)$, which are functions of the external magnetic field, are the rate constants of the triplet–doublet quenching (T–D quenching) process and the T–T annihilation process, respectively. Because the lifetime of the TMPD cation radical is much longer than that of the excited triplet state (T_1) of TMPD,^{9,18} the T–D quenching process can be expressed by a pseudo-first-order reaction with the rate constant $k_3''(B)$ expressed by $k_3''(B) = k_3'(B)[D]$. The set of differential equations for the model represented by Scheme 1 is

$$\frac{d[S_1]}{dt} = -(K_1 + k_2)[S_1] + k_4(B)[T_1]^2 \quad (3)$$

$$\frac{d[T_1]}{dt} = k_2[S_1] - K_3(B)[T_1] - 2k_4(B)[T_1]^2 \quad (4)$$

where

$$K_1 = k_1 + k_1^* + k_1' \quad (5)$$

$$K_3(B) = k_3 + k_3^* + k_3''(B) \quad (6)$$

Equations 3 and 4 lead to the delayed fluorescence intensity via T–T annihilation

$$I(B) = I_0(B) \exp[-2K_3(B)t] \quad (7)$$

where

$$I_0(B) = \frac{k_1^*k_2^2k_4(B)R_0^2}{(K_1 + k_2)^2} \quad (8)$$

and R_0^2 is a function of the conditions on excitation.¹⁹ Finally, the equation that shows the time evolution of the intensity ratio

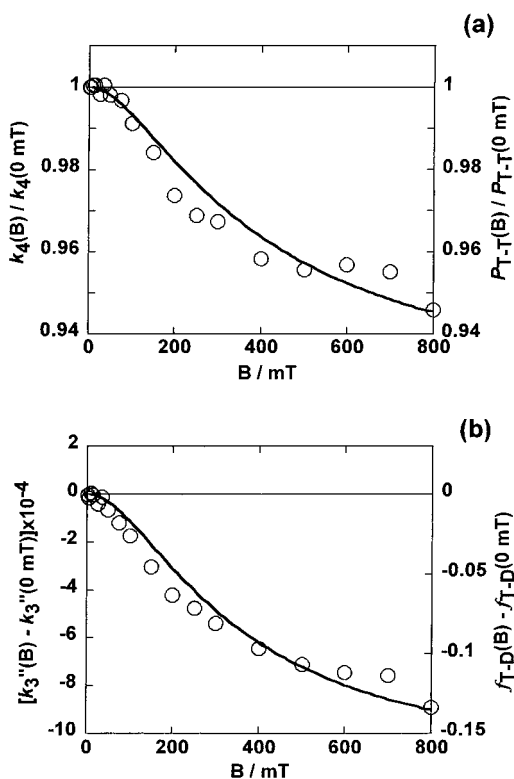


Figure 4. Magnetic field dependence of (a) $k_4(B)/k_4(0 \text{ mT})$ and (b) $k_3''(B) - k_3''(0 \text{ mT})$. The open circles show the magnetic field dependence derived from the experimental data. The solid lines show the magnetic field dependence calculated by eq 12. (See text)

on the T–T annihilation type of delayed fluorescence, $[I(B) - I(0 \text{ mT})]/I(0 \text{ mT})$, is expressed by

$$\begin{aligned} \frac{I(B) - I(0 \text{ mT})}{I(0 \text{ mT})} &= \frac{k_4(B)}{k_4(0 \text{ mT})} \exp\{-2[K_3(B) - K_3(0 \text{ mT})]t\} - 1 \\ &= \frac{k_4(B)}{k_4(0 \text{ mT})} \exp\{-2[k_3''(B) - k_3''(0 \text{ mT})]t\} - 1 \end{aligned} \quad (9)$$

Equation 9 indicates that a distinction between the MFEs due to the TTPM and the TDPM can be made on the basis of the observation data. The analysis of the observed time evolution of the MFE at every magnetic field by curve fitting according to eq 9 can lead to an experimental preexponential value of $k_4(B)/k_4(0 \text{ mT})$ and the exponential part of $k_3''(B) - k_3''(0 \text{ mT})$. The dotted line in Figure 3a shows the curve fitting result obtained at 800 mT in this manner. The circles in Figure 4a and 4b show the MFE curves of the experimental value of $k_4(B)/k_4(0 \text{ mT})$ and $k_3''(B) - k_3''(0 \text{ mT})$, respectively. The fact that $k_4(B)/k_4(0 \text{ mT})$ is less than unity shows that the T–T annihilation process is decelerated by the application of a magnetic field, which is to say, the intensity of the T–T annihilation type of delayed fluorescence under a magnetic field is weaker than that at zero magnetic field. Therefore, this characteristic of $k_4(B)/k_4(0 \text{ mT})$ corresponds to the negative sign of the MFE in the early-time region in Figure 3b. The negative sign of $k_3''(B) - k_3''(0 \text{ mT})$ shows that the T–D quenching process is decelerated by the application of a magnetic field, specifically, the T_1 state of TMPD under magnetic field has a longer lifetime than it does at zero magnetic field. Therefore, the intensity of the T–T annihilation type of delayed fluorescence, which is proportional to $[T_1]^2$, increases with increasing magnetic field. This charac-

teristic of $k_3''(B) - k_3''(0 \text{ mT})$ also corresponds to the positive sign of the MFE in the later-time region as shown in Figure 3b. Furthermore, these tendencies correspond to those of the TTPM and the TDPM discussed in the previous papers.^{1,3,4,20–26}

We calculated the magnetic field dependences of $k_4(B)/k_4(0 \text{ mT})$ and $k_3''(B) - k_3''(0 \text{ mT})$ according to the analytical methods proposed by Atkins et al.²⁷ These methods involve simple quantum-mechanical calculations including relaxation due to only intradipole interactions of the triplet molecules. We consider a T–T pair composed of two T_1 molecules of TMPD and a T–D pair composed of a T_1 molecule of TMPD and a TMPD cation radical. Assuming that the g values of two T_1 molecules in the T–T pair and of the T_1 molecule and the TMPD cation radical in the T–D pair are isotropic and identical, $g = g_T = g_D = 2$, the spin Hamiltonians are as follows:

$$H_{T-T} = g\mu_B B \hbar^{-1} (S_{T1Z} + S_{T2Z}) - 2JS_{T1}S_{T2} - \sum_{i=1,2} S_{Ti} D(\Omega_{Ti}) S_{Ti} \quad (10a)$$

$$H_{T-D} = g\mu_B B \hbar^{-1} (S_{TZ} + S_{DZ}) - 2JS_T S_D - S_T D(\Omega) S_T \quad (10b)$$

The T–T annihilation and the T–D quenching occur from the singlet state (S) of the T–T pair and the doublet state ($D_{\pm 1/2}$) of the T–D pair, respectively. Therefore, the rate constants of the T–T annihilation and T–D quenching, $k_4(B)$ and $k_3''(B)$, respectively, are proportional to the T–T annihilation and T–D quenching probabilities, $P_{T-T}(B)$ and $P_{T-D}(B)$, respectively

$$k_4(B) \propto P_{T-T}(B) = \lambda_T [1 - \lambda_T + \lambda_T f_{T-T}(B)] \quad (11a)$$

$$k_3''(B) \propto P_{T-D}(B) = 1 - \frac{1}{3}\lambda_D + \lambda_D^2 - \lambda_D^2 f_{T-D}(B) \quad (11b)$$

where $f_{T-T}(B)$ and $f_{T-D}(B)$ are the parameters related to the singlet character in the T–T pair and doublet character in the T–D pair, respectively, as shown in Appendix. λ_T and λ_D are the reaction probabilities from the singlet state of the T–T pair and the doublet state of the T–D pair, respectively. Finally, the equations that show the MFEs due to the T–T pair and the T–D pair are expressed as

$$\frac{k_4(B)}{k_4(0 \text{ mT})} = \frac{P_{T-T}(B)}{P_{T-T}(0 \text{ mT})} = \frac{1 + \phi_{T-T} f_{T-T}(B)}{1 + \phi_{T-T} f_{T-T}(0 \text{ mT})} \quad (12a)$$

$$\begin{aligned} k_3''(B) - k_3''(0 \text{ mT}) &\propto P_{T-D}(B) - P_{T-D}(0 \text{ mT}) \\ &\propto f_{T-D}(B) - f_{T-D}(0 \text{ mT}) \end{aligned} \quad (12b)$$

where

$$\phi_{T-T} = \frac{\lambda_T}{1 - \lambda_T} \quad (13)$$

Simple conceptual diagrams of the T–T and T–D pairs are shown in Figures 5a and 5b, respectively. Because the population transfer between the quintet and the singlet states in the T–T pair is decelerated by the Zeeman splitting of the spin states with increasing external magnetic field, the intensity of the delayed fluorescence decreases at high magnetic field. In the T–D pair, the deceleration of quenching of the pair can be explained in the same manner. The solid lines in Figure 4a and 4b show the calculated MFE curves due to the T–T and T–D pairs according to eqs 12a and 12b, respectively. The parameters used here are shown in Table 1. $\lambda_T = 0.25$ is a reasonable value according to the demonstration by Atkins et al.²⁷ As shown in

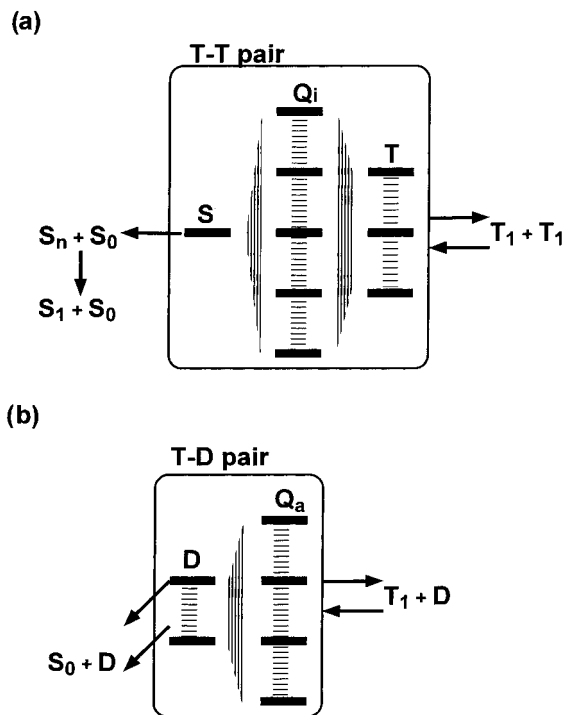


Figure 5. Conceptual diagrams of the MFEs due to the TTPM and the TDPM. (a) The T–T pair is created by the random encounter of two triplet molecules. The T–T annihilation process occurs through the singlet state (S) of the T–T pair. (b) The T–D pair is created by the random encounter of a triplet molecule and a radical. The T–D quenching process occurs through the doublet state of the T–D pair. The population transfer between the different spin multiplicity states in the pairs occurs by intradipole interactions of the triplet molecule.

TABLE 1: Parameters for the Calculation of the MFEs Due to the TTPM and the TDPM

zero-field splitting constants of the lowest excited triplet TMPD ²⁸ (cm ⁻¹)	
$D = 0.0506, E = -0.035$	
diffusion coefficient ²⁹ (m ² s ⁻¹)	
excited triplet TMPD	1.8×10^{-9}
TMPD cation radical	0.91×10^{-9}
viscosity ^{30–32} (cP)	
2-propanol	1.8
mixed alcohol	2.6
reaction probability of the T-T pair	
λ_T	0.25

Figure 4a and 4b, both calculated MFE curves reproduce the observed data well. The negative MFEs observed for both concentrations and the positive MFE observed in the later-time region under high-concentration conditions can be explained by the TTPM and the TDPM, respectively.

Accordingly, the delayed fluorescence in the present system is classified into two emission mechanisms, recombination and T–T annihilation. The observation of the MFE due to the TDPM indicates the importance of the T–D pair in this particular system for the first time.

In 2-Propanol Solution. Under low-concentration conditions, no obvious positive MFE due to the RPM was observed within our experimental inaccuracy, but a negative MFE of about 8% at 1.2 T was observed clearly. No apparent observation of the MFE arising from the RPM might be due to the low viscosity and/or high permittivity of the solvent. According to eq 8, the initial delayed fluorescence intensity due to T–T annihilation is proportional to the rate constant of the T–T annihilation process, $k_4(B)$, which is a diffusion-controlled reaction. Because the viscosity of 2-propanol (1.8 cP) is less than that of the mixed

TABLE 2: Mechanisms of the MFE Observed in Mixed Alcohol and 2-Propanol Solution of TMPD

	low concentration		high concentration	
	early time	later time	early time	later time
mixed alcohol	RPM	TTPM	TTPM	TDPM
2-propanol	TTPM	TTPM	TTPM	TDPM

alcohol (2.6 cP) under our experimental conditions,^{30–32} the delayed fluorescence intensity due to the T–T annihilation in 2-propanol might be stronger than that in the mixed alcohol. The permittivities of the solvents [$\epsilon_r(2\text{-propanol}) = 19.92$ and $\epsilon_r(2\text{-methyl-2-propanol}) = 12.47$ at 25 °C]³² might affect the charge recombination efficiency. The rate constant of back electron transfer from the singlet RIP to S₁, which determines the intensity of the recombination-type delayed fluorescence, might depend on the permittivity of the solvent. Consequently, the signal of the recombination-type delayed fluorescence might be obscured by the intense signal of the T–T annihilation type of delayed fluorescence in 2-propanol. This might have prevented Sacher's group¹⁶ from observing the MFE on the delayed fluorescence in this particular system by using a modulated magnetic field. However, the existence of the RPM in 2-propanol has already been demonstrated by microwave nutation experiments in more diluted solutions.^{12,15}

Under high-concentration conditions, the MFEs are very similar to that observed under high concentration in the mixed alcohol solution. Therefore, the MFEs in the 2-propanol solution can be explained by the same manner as that in the mixed alcohol solution.

Conclusion

We succeeded in clarifying the emission mechanism of the delayed fluorescence and the mechanism of the MFEs on the delayed fluorescence according to the time-domain observation of the MFEs in the photochemical system of TMPD. The delayed fluorescence in the present unique system shows three types of MFEs, which can be attributed to the RPM, TTPM, and TDPM, as shown in Table 2. These MFEs make it clear that both the recombination and the T–T annihilation types of delayed fluorescence emit and that the lowest excited triplet of TMPD is quenched by the TMPD cation radical. Here, it is noteworthy that three different MFEs are observed by time-domain measurements in nonviscous solutions at room temperature and that these MFE results clarify the mechanisms of the delayed fluorescence. The time-domain observation of MFEs is shown to be a useful technique for investigating the paramagnetic pairs involved in photochemical reactions in liquid media. It is shown that the spin behavior of not only the radical pair but also the T–T and T–D pair plays an important role in the photochemical reaction.

Acknowledgment. Authors express their grateful acknowledgment to Professor T. Azumi for stimulating discussions. This work was supported by a Grant-in-Aid on Priority-Area-Research on Photoreaction Dynamics (08218205) and a Grant-in-Aid for Development Science Research (08740437, 10440164) from the Ministry of Education, Science, Sports and Culture of Japan.

Appendix

The parameters $f_{T-T}(B)$ and $f_{T-D}(B)$ in eqs 11a and 11b are given by²⁷

$$f_{T-T}(B) = \frac{1}{9} \{ 8 - [F(6R_{1100}) + F(2W_{1T}) + 2F(-2R_{1-11-1}) + 2F(2W_{2T}) + 2F(2R_{1010} - 2R_{100-1})] \} \quad (\text{A1a})$$

$$f_{T-D}(B) \approx \frac{1}{9} \{ 6 - 2[F(W_{1T}) + 2F(W_{2T})] \} \quad (\text{A1b})$$

and at zero field

$$f_{T-T}(0 \text{ mT}) = \frac{8}{9} - \frac{5}{9} F \left[\frac{4}{5} k(0 \text{ mT}) \right] - \frac{1}{3} F \left[\frac{4}{3} k(0 \text{ mT}) \right] \quad (\text{A1c})$$

$$f_{T-D}(0 \text{ mT}) = \frac{2}{3} \{ 1 - F[k(0 \text{ mT})] \} \quad (\text{A1d})$$

where

$$F(s) = \frac{\sinh[(s\tau_a)^{1/2}] \exp[-(s\tau_a)^{1/2}]}{(s\tau_a)^{1/2}} \quad (\text{A2})$$

$$\tau_{a,T-T} = \frac{2r_T^2}{D_T} \quad (\text{A3a})$$

$$\tau_{a,T-D} = \frac{(r_T + r_D)^2}{D_T + D_D} \quad (\text{A3b})$$

$$W_{1T} = R_{1100} + R_{11-1-1} \quad (\text{A4})$$

$$W_{2T} = -R_{1010} + R_{100-1} \quad (\text{A5})$$

$R_{mm'mm'}$ and $k(0 \text{ mT})$ are presented in the equations given later. τ_a is the translational correlation time, and r_T and r_D are the radii of the triplet and doublet molecules, respectively. D_T and D_D are the translational diffusion constants of the triplet and doublet molecules, respectively. In the present numerical calculations, the radius of the excited triplet TMPD, r_T , is assumed to be the same as that of the TMPD cation radical, r_D , and it is estimated from D_D by the Stokes–Einstein relation.²⁹ W_{1T} and W_{2T} are the reciprocal of the longitude relaxation time and the reciprocal of the transverse relaxation time, respectively. $R_{mm'mm'}$ is the Redfield relaxation matrix given by

$$R_{1100} = \frac{2}{15} k(B) \quad (\text{A6})$$

$$R_{11-1-1} = \frac{4}{15} k(2B) \quad (\text{A7})$$

$$R_{1010} = -\frac{1}{5} [k(0 \text{ mT}) + k(B) + \frac{2}{3} k(2B)] \quad (\text{A8})$$

$$R_{100-1} = -\frac{2}{15} k(B) \quad (\text{A9})$$

$$R_{11-1-1} = -\frac{2}{15} [k(B) + 2k(2B)] \quad (\text{A10})$$

where

$$k(B) = \frac{(D^2 + 3E^2)\tau_2}{1 + (g\mu_B B \hbar^{-1} \tau_2)^2} \quad (\text{A11a})$$

$$k(0 \text{ mT}) = (D^2 + 3E^2)\tau_2 \quad (\text{A11b})$$

$$\tau_2 = \frac{1}{6D_r} \quad (\text{A12})$$

τ_2 is the rotational correlation time, and D_r is the rotational diffusion constant of the triplet molecule, with isotropic rotational diffusion assumed. τ_a is connected to τ_2 by the Stokes–Einstein relation, $\tau_a = 9\tau_2$.

References and Notes

- (1) Steiner, U. E.; Ulrich, T. *Chem. Rev.* **1989**, *89*, 51.
- (2) Hayashi, H.; Sakaguchi, Y. *Lasers in Polymer Science and Technology: Applications*; Fouassier, J.-P., Rabek, J. F., Eds.; CRC Press: Boca Raton, FL, 1990; Vol. II, Chapter 1.
- (3) Parker, C. A. *Photoluminescence of Solution*; Elsevier: Amsterdam, 1968;
- (4) Geacintov, N. E.; Swenberg, C. E. *Luminescence Spectroscopy*; Lumb, M. D., Ed.; Academic Press: London, 1978; Chapter 2.
- (5) *The Triplet State*; Zahlan, A. B., Androes, G. M., Hutchison, C. A., Jr., Hameka, H. F., Robinson, G. W., Heineken, F. W., van der Waals, J. H., Eds.; Cambridge University Press: Cambridge, U.K., 1967.
- (6) McGlynn, S. P.; Azumi, T.; Kinoshita, M. *Molecular Spectroscopy of the Triplet State*; Prentice Hall: New York, 1969.
- (7) Ottolenghi, M. *Chem. Phys. Lett.* **1971**, *12*, 339.
- (8) Hirata, Y.; Mataga, N. *J. Phys. Chem.* **1983**, *87*, 3190.
- (9) Hirata, Y.; Mataga, N. *J. Phys. Chem.* **1985**, *89*, 4031.
- (10) Tanimoto, Y.; Watanabe, T.; Nakagaki, R.; Hiramatsu, M.; Nagakura, S. *Chem. Phys. Lett.* **1985**, *119*, 341.
- (11) Murai, H.; Matsuyama, A.; Ishida, T.; Iwasaki, Y.; Maeda, K.; Azumi, T. *Chem. Phys. Lett.* **1997**, *264*, 619.
- (12) Murai, H.; Matsuyama, A.; Iwasaki, Y.; Enjo, K.; Maeda, K.; Azumi, T. *Appl. Magn. Reson.* **1997**, *12*, 411.
- (13) Percy, L. T.; Bakker, M. G.; Trifunac, A. D. *J. Phys. Chem.* **1989**, *93*, 4393.
- (14) Bakker, G.; Trifunac, A. D. *J. Phys. Chem.* **1991**, *95*, 550.
- (15) Iwasaki, Y.; Murai, H.; Maeda, K.; Azumi, T. *Chem. Phys.* **1998**, *230*, 201.
- (16) Sacher, M.; Grampp, G. *Ber. Bunsen-Ges. Phys. Chem.* **1997**, *101*, 971.
- (17) Werner, H.-J.; Staerk, H.; Weller, A. *J. Chem. Phys.* **1978**, *68*, 2419.
- (18) Isaka, H.; Suzuki, S.; Ohzeki, T.; Sakaino, Y.; Takahashi, H. *J. Photochem.* **1987**, *38*, 167.
- (19) Azumi, T.; McGlynn, S. J. *Chem. Phys.* **1963**, *39*, 1186.
- (20) Faulkner, L. R.; Bard, A. J. *J. Am. Chem. Soc.* **1969**, *91*, 6495.
- (21) Faulkner, L. R.; Bard, A. J. *J. Am. Chem. Soc.* **1969**, *91*, 209.
- (22) Faulkner, L. R.; Tachikawa, H.; Bard, A. J. *J. Am. Chem. Soc.* **1972**, *94*, 691.
- (23) Tachikawa, H.; Bard, A. J. *Chem. Phys. Lett.* **1973**, *19*, 287.
- (24) Tachikawa, H.; Bard, A. J. *Chem. Phys. Lett.* **1974**, *26*, 246.
- (25) Faulkner, L. R.; Bard, A. J. *J. Am. Chem. Soc.* **1969**, *91*, 6497.
- (26) Tachikawa, H.; Bard, A. J. *Chem. Phys. Lett.* **1974**, *26*, 246.
- (27) Atkins, P. W.; Evans, G. T. *Mol. Phys.* **1975**, *29*, 921.
- (28) Matsui, K.; Morita, H.; Nishi, N.; Kinoshita, M.; Nagakura, S. *J. Chem. Phys.* **1980**, *73*, 5514.
- (29) Terazima, M.; Okazaki, T.; Hirota, N. *J. Photochem. Photobiol. A* **1995**, *92*, 7.
- (30) Kitahama, Y.; Murai, H. *Chem. Phys.* **1998**, *238*, 429.
- (31) Ishikawa, T. *Kongou-eki Nendo no Riron*; Maruzen: Tokyo, Japan, 1968.
- (32) Riddick, J. A.; Bunger, W. B. *Organic Solvents*, 3rd ed.; Wiley-Interscience: New York, 1970.